

# Effect of Self-Pouring Temperature on the Microstructural Characteristics of Al<sub>2</sub>O<sub>3</sub>-LM6 Semi-solid Cast Composite

Devendra Pratap Singh<sup>1</sup> · Vijay Kumar Dwivedi<sup>1</sup> ·  
Mayank Agarwal<sup>2</sup>

Received: 8 January 2024 / Accepted: 28 March 2024  
© The Institution of Engineers (India) 2024

**Abstract** The influence of self-pouring temperature condition was used to convert Al<sub>2</sub>O<sub>3</sub> and LM6 powder particles into a cast composite. In comparison with a conventional casting process, a modified route for fabrication of the Al<sub>2</sub>O<sub>3</sub>-LM6 composite was used under low pressure compaction and furnace heating. In this experimental work, ball-milled powder particles were compacted with the effect of heat flowing through a tapered passage in a die under gravitational flow action. The microstructure evaluation and mechanical properties of the produced composite were investigated for the developed composite. The observation of the microstructure and mechanical properties reveals successful incorporation of the reinforcement which significantly improved the mechanical properties and cast microstructure. The results suggest that maximum possibility of improvement in mechanical properties is obtained for the mixture combination of 83.5% Al blended with 12.5% Si and 4% Al<sub>2</sub>O<sub>3</sub> by wt. Increments of 0.36%, 5.57%, and 5.23% in the density, hardness, and impact strength, respectively, were observed, which was also identified in the analysis of variance of the experimental data for the interaction effect of each processing parameter.

**Keywords** Al<sub>2</sub>O<sub>3</sub> · LM6 · Self-pouring temperature · Microstructure · Cast-composite

## Introduction

In ceramics, aluminum oxide (Al<sub>2</sub>O<sub>3</sub>) is a most renowned and acceptable for its easy use and availability. Al<sub>2</sub>O<sub>3</sub> is widely used in the aerospace components, automotive utilities, and medical appliances due to its excellent hardness, chemical and mechanical properties, and forming qualities. Also, biocompatibility and formability of Al<sub>2</sub>O<sub>3</sub> make it perfect for medical implants, insulators and ceramic-based utilities. Aluminum-based metal matrix composites are widely used in various engineering applications such as automobile, aerospace, household utilities like panels, metal furniture, stairs, structural members for these composites. Several modifications have been considered according to the type of reinforcement selection and processing techniques along with associated parameters of casting [1–5]. In comparison with the large-sized reinforcement particles, fine and micro-sized reinforcement particles have a great ability to enhance the mechanical properties due to the interfacial strength developed in between the reinforcement and matrix. For this purpose, micro-sized alumina particles are considered for an Al<sub>2</sub>O<sub>3</sub>-Al matrix composite due to the excellent level of compatible mixing during the semi-solid casting process [6, 7]. Generally, LM6 alloy is known as piston alloy with higher alloying of silicon content (~10–13%) and with its excellent flexibility. Moreover, LM6 is considered in industries for the fabrication due to its greater wear and higher corrosive resistance [8, 9]. On the other hand, products developed by semi-solid casting processes up to a certain extent provide excellent properties [10–18]. Continuous changes and modifications are always required in industries fabricating products from aluminum to avoid any type of casting defects such as porosity, void formation, mismatch shrinkage behavior. For this purpose, changes are suggested regarding selection of the materials

✉ Mayank Agarwal  
mayankres@gmail.com

<sup>1</sup> Institute of Engineering Technology, GLA University,  
Mathura 281406, India

<sup>2</sup> Institute of Engineering Technology, Dr. Ram Manohar  
Lohia Avadh University, Ayodhya 224001, India

and the processing technique. In the processing technique, temperature is an important processing parameter to control the constraints and other associated parameters reported by several authors [18]. Nonetheless, control of the pouring temperature is a key candidate for the various changes and modifications with material incorporation method during the synthesis of ceramic-based composites [19–22].

The impact of a novel metal processing route for the fabrication of the  $\text{Al}_2\text{O}_3$ -LM6 composite has been represented in this experimental work. With an identification of self-pouring condition for the bulk material, without any use of slurry formation, approach suggested possible unique solution for composite development. Notably, a consolidated effect of self-pouring temperature and  $\text{Al}_2\text{O}_3$  on the casting process adds a novel possibility to traditional and advanced casting techniques. However, in this work, impact of self-pouring temperature and  $\text{Al}_2\text{O}_3$  is considered for the synthesis of  $\text{Al}_2\text{O}_3$ /LM6 semi-solid cast composite along with microstructural and mechanical evaluation.

## Materials and Method

### Material Selection and Preparation

LM6 powder (180 mesh, mean diameter  $D=0.076$  mm, density =  $2.66 \text{ g/cm}^3$ ) was chosen as the matrix material, while  $\text{Al}_2\text{O}_3$  particles (120 mesh, mean diameter  $D=0.13$  mm, density =  $3.95 \text{ g/cm}^3$ ) were utilized for reinforcement. These materials were sourced from Loba Chemie Pvt. Ltd. The powders were pre-heated in a 220–230 V hot-air electric oven at  $50^\circ\text{C}$  for 30 min before being mixed via ball milling in a 1:10 powder to ball weight ratio with the addition of 1 g of graphite for dry lubrication. The mixing process occurred at 50 rpm in three rounds of 40 min each, followed by a cooling-off time of 20 min. The microstructure of the moisture-free mixed powder revealed the hexagonal shape of the alumina particles (size  $< 20 \mu\text{m}$ ) and the LM6 powder containing brittle silicon asperities (size  $< 40 \mu\text{m}$ ) intermixed with  $\text{Al}_2\text{O}_3$  particles.

### Fabrication Process

The ball-milled mixture of  $\text{Al}_2\text{O}_3$  and LM6 powder was then compressed inside a closed die with a chrome-plated cavity using a spring compaction machine (Make: ATS BHI100; year 2018) under an applied load of 1.8 kN. The pre-forms were held inside a warm air chamber at a constant temperature of  $30^\circ\text{C}$  for approximately 24 h before being taken out from the die cavity for further processing. Twelve pre-forms were arranged on the upper side of a Plaster of Paris (POP) die inside a muffle furnace (Make: KS1200 4.0 kW) for heating in an argon environment to avoid oxidation. The middle

part of the POP die was tapered to assist the gravitational flow of the melted pre-form at a specific temperature range established for smooth flow.

### Flow Behavior and Casting

During the milling process, ductile Al clustered by 15–17% of brittle ceramic was crushed into smaller-sized particles, enhancing the heat transfer rate. The melted pre-forms were dripped into the POP die cavity at the lower portion to produce the final cast product. A digital pyrometer with an accuracy of  $\pm 5^\circ\text{C}$  was used to monitor the temperature during the entire process. The experimental setup facilitated the initiation of the liquid phase while the bulk remained primarily solid, with only the low-density Al powder particles melting initially. This resulted in a uniform flow behavior, akin to conventional slurry flow but at a lower melting temperature (Involved steps are represented in Fig. 1).

### Material Characterization

Microstructure analysis (Make: ZEISS, SUPRA 40 VP) at various locations of the cast composite was performed to assess the surface-level effects of the sequential processing steps. Impact strength was evaluated via Charpy impact testing according to ASTM-E23 and ISO 148-1 standards. Specimens were prepared and tested using an impact testing machine (Make: TM232 25/50J). The average density was measured according to the Archimedes principle (ASTM B328). Brinell hardness testing was conducted on prepared specimens as per ASTM E10-18 standards using a hardness testing machine (Make: Saroj, B-3000 (H)). XRD evaluation was carried out using a PANalytical X'Pert X-Ray Diffractometer to identify phases and elemental components, collecting peak values over a  $2\theta$  range of  $10^\circ$ – $90^\circ$  with a step size of  $0.1^\circ$ .

## Result and Discussion

Mechanical characteristics of developed  $\text{Al}_2\text{O}_3$ -LM6 cast composite under self-pouring temperature condition has been summarized in Table 1 for various combination of  $\text{Al}_2\text{O}_3$  and LM6 powder particulates. Accordingly, Table 1 density and hardness value increase as a function of the  $\text{Al}_2\text{O}_3$  addition amount which was well expected [7, 21].

On the other hand, not much of a significant difference is observed in the values of impact strength of composite for the addition of  $\text{Al}_2\text{O}_3$ . The obtained results for hardness and impact strength of the  $\text{Al}_2\text{O}_3$ -LM6 powder composite are significantly influenced by various processing parameters. Specifically, the self-pouring temperature plays a crucial role

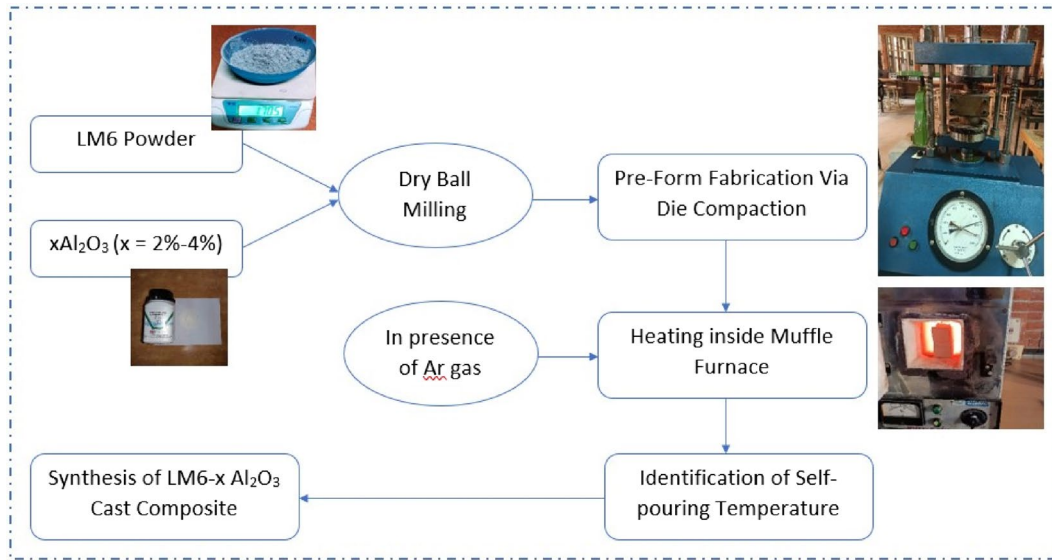


**Fig. 1** Processing steps involved in development of  $\text{Al}_2\text{O}_3$ -LM6 self-pouring temperature composite

**Table 1** Mechanical characteristics of developed  $\text{Al}_2\text{O}_3$ -LM6 composite

S. no.	Material combination	Density ( $\text{g}/\text{cm}^3$ )	BHN	Impact strength ( $\text{kJ}/\text{m}^2$ )	Self-pouring temperature ( $^\circ\text{C}$ )
1	LM6- $\text{Al}_2\text{O}_3$ (2%)	2.68	86.1 (range; 85.8–86.4)	14.23 (range; 13.9–14.7)	649.9 (range; 642–657)
2	LM6- $\text{Al}_2\text{O}_3$ (3%)	2.69	90.9 (range; 90.6–91.2)	13.94 (range; 13.6–14.2)	665.7 (range; 661–670)
3	LM6- $\text{Al}_2\text{O}_3$ (4%)	2.71	94.2 (range; 93.7–94.3)	14.67 (range; 14.2–15.1)	690.7 (range; 686–695)

for the determination the flow behavior and distribution of reinforcement particles within the LM6 matrix, with optimal temperatures enhancing mechanical properties. According to the microstructure of impact fractured surfaces shown in Fig. 2d–f, it is clearly visible that embedded  $\text{Al}_2\text{O}_3$  particulates used in the process are plucked out and due to this, the formation of cavities (red circle, Fig. 2d) from the surface, while some structured combined mixed reinforcement particulates are observed in Fig. 2e. A similar effect for the particles is also found in Fig. 2f for 4%  $\text{Al}_2\text{O}_3$  addition but in a slightly different way. Here, particles were settled near the available spaces in between grains. According to Fig. 2e, this might be represented those brittle particles were plucked out differently for the presence of an interfacial layer of  $\text{Al}_2\text{O}_3$  and Al content. According to the obtained experimental data, it is observed that hardness is a parallel component for the improvement in the other properties with respect to the density with addition of  $\text{Al}_2\text{O}_3$ . It is well known that density and hardness of  $\text{Al}_2\text{O}_3$ , both are higher with respect to parent material and this compositional increase in the properties was well expected. This might be possible due to the low self-pouring temperature condition which affects the solidification rate. Due to the effect of these interfacial

layers, the tendency of brittle particles is not similar to the conventional casting process [8, 17, 23].

Cast microstructure for  $\text{Al}_2\text{O}_3$  modified LM6 alloy composite fabricated under a self-pouring temperature range of 650–700  $^\circ\text{C}$  for different combinations of  $\text{Al}_2\text{O}_3$  powder particulates is shown in Fig. 3. The distribution of  $\text{Al}_2\text{O}_3$  is well affected by the amount of addition of powder particles (reinforcement) and is considered a function of pouring temperature [24]. The individual effect of  $\text{Al}_2\text{O}_3$  and self-pouring temperature on the  $\text{Al}_2\text{O}_3$ -LM6 composite is discernible from the observed mechanical characteristics.  $\text{Al}_2\text{O}_3$  addition influences properties such as density and hardness positively, with an increase correlating with the amount of added  $\text{Al}_2\text{O}_3$ . As well as self-pouring temperature affects the flow behavior and solidification rate of the composite, impacting its microstructure and mechanical properties. The optimum self-pouring temperature for the 4%  $\text{Al}_2\text{O}_3$ -LM6 composite is found to be 690.7  $^\circ\text{C}$ . Both processing parameters and reinforcement amount play crucial. Therefore, both factors must be carefully controlled and optimized to achieve desired mechanical properties. Segregation of the particles of  $\text{Al}_2\text{O}_3$  near the grain boundaries of solidified LM6 matrix shows that incorporation of these particles takes place inside the micro pores and cavities [9]. This is a bigger

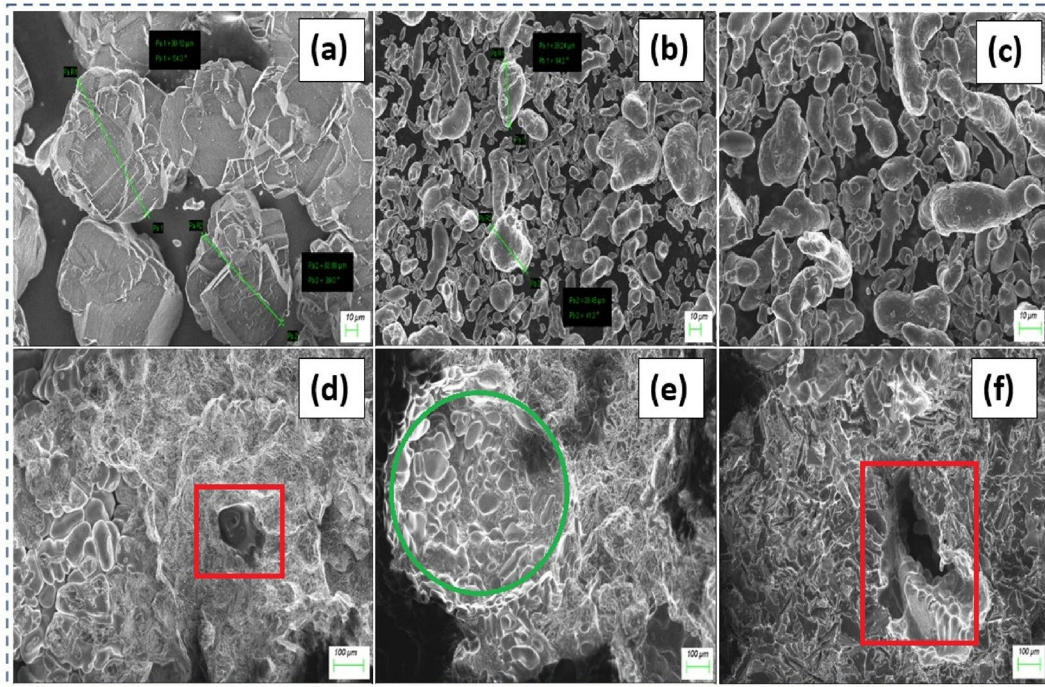


**Fig. 2** Morphology for **a** powder particle of  $\text{Al}_2\text{O}_3$ ; **b** powder particle of LM6; **c** Ball milled Powder particles of  $\text{Al}_2\text{O}_3$  and LM6; morphology of impact fractured surface **d** 2%  $\text{Al}_2\text{O}_3$  addition; **e** 3%  $\text{Al}_2\text{O}_3$  addition; **f** 4%  $\text{Al}_2\text{O}_3$  addition (Color figure online)

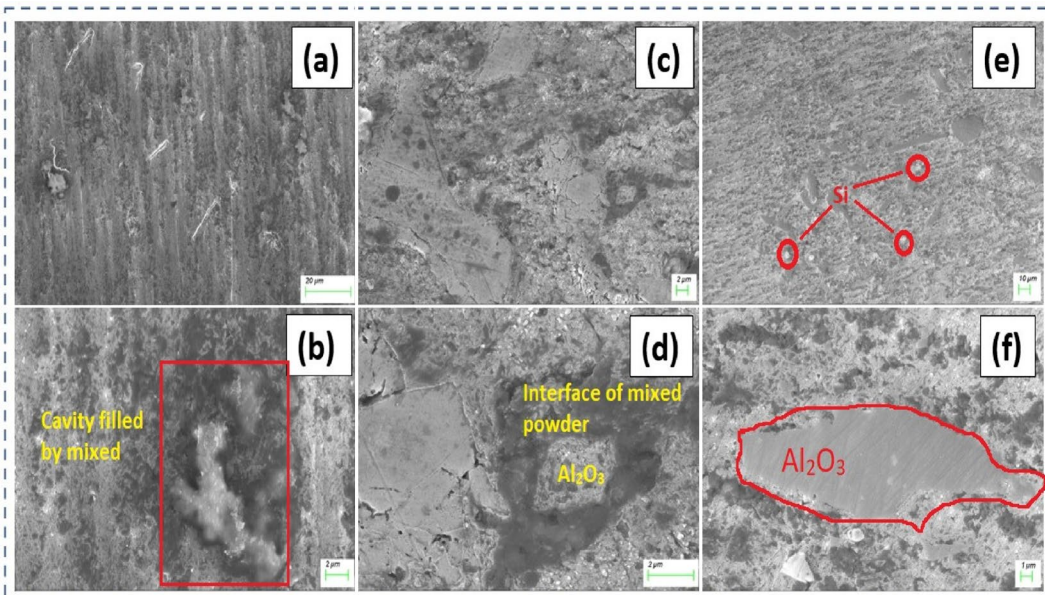


**Fig. 3** Microstructure for the **a, b** 2%  $\text{Al}_2\text{O}_3$ -LM6 composite; **c, d** 3%  $\text{Al}_2\text{O}_3$ -LM6 composite; **e, f** 4%  $\text{Al}_2\text{O}_3$ -LM6 composite

challenge for a proper mixing of powder particles with different densities and properties. Here, LM6 and  $\text{Al}_2\text{O}_3$  both are compatible to each other according to the mixing due to the presence of Al powder particles (approx. 85%). This combination provides ability to provide an initial joining

and mixing during the milling process. Although, melting temperature of the particle is different but, in this work, flow behavior and melting is governed by the Al powder particles (primary processing component), while un-melted brittle Si and  $\text{Al}_2\text{O}_3$  particulates are joined with generated interfaces

during the solidification. The settlement of un-melted solid particles inside the cavity can be attributed to several factors. During the heating process, as the temperature rises, binding strength of the green compact is lost, leading to the initiation of melting for the outer layer. Continuous heating affects the heat transfer rate, resulting in the generation of liquid vapor bubbles of aluminum at various locations within the green compact. These bubbles facilitate the flow of brittle particulates, such as Si present in LM6 and  $\text{Al}_2\text{O}_3$  hexagonal ceramic particles. As a result, larger cavities are formed, where clustered  $\text{Al}_2\text{O}_3$  particles settle, surrounded by aluminum in the LM6 alloy and its inter-phases. This might be an effect of the flow condition of the melt and higher density of  $\text{Al}_2\text{O}_3$  particles as comparison to the LM6 powder particle. Further, with decrease in the amount of LM6, flow velocity of the melted mixed green compact is also reduced. During melting, bigger size powder particles were floated inside the bigger cavities which were generated during the solidification as found in Fig. 3f. The effect of powder particle size on the  $\text{Al}_2\text{O}_3$ -LM6 composite properties is evident in the observed microstructure and mechanical characteristics. Bigger size powder particles tend to float inside the bigger cavities generated during solidification, leading to non-uniform distribution within the cast microstructure. This uneven distribution affects the mechanical properties of the composite, particularly impacting factors like hardness and density. A similar effect is also observed for 2% and 3% addition of  $\text{Al}_2\text{O}_3$  (as shown in Fig. 3b, d, but the size of the bigger particles is observed in Fig. 3f). On the other hand, Fig. 3a, c and e represents the distribution of reinforcement particulates throughout the cast microstructure, which is absent in a particular cluster zone. This distribution of the particles along the matrix and reinforcement regimes is affected by solidification behavior and the type of interface zone [7, 25]. This also is a result of incomplete recrystallization and thermal mismatch during the heating of the powder particulate ( $\text{Al}_2\text{O}_3$  and LM6) [25]. Generally, primary shrinkage appears on the matrix and softer phases while secondary shrinkage (for higher temperature range) is required for reinforcement. Moreover, generated interfacial phases during this stage, interfacial energy of the reinforcement vapor is converted to heat. This energy might be transferred to the metal reinforcement interfacial energy during the early instant of the solidification. In this experimental work, although the flow of the metals starts near about 700 °C, but solidification is started first due to fine powder particles and higher surface area [2, 22, 25].

During heating, binding strength of the green compact was lost with the rise in the temperature of furnace which propagated the starting of melting for outer layer of green compact. Further, continuous heating affects the heat transfer rate, and progressively some amount of porosity with the liquid vapor of aluminum, which is generated at various

locations of the green compact. The process, results in the drop in conductive heat transfer of the compact block. Along with this aspect, size of the liquid vapor bubble of the aluminum particle is increases continuously which helps to flow of the brittle particulates (Si present in LM6 and  $\text{Al}_2\text{O}_3$  hexagonal ceramic particles) [7, 26]. Finally, result of this effect provides an early flow of aluminum particles rather than present brittle particles [27]. This is clearly observed (Fig. 3f and d) that clustered  $\text{Al}_2\text{O}_3$  bigger particles are settled inside the bigger size cavities. These cavities are surrounded by present aluminum in LM6 alloy and its inter-phases [9, 17, 26]. Moreover, amount of micro-size Si brittle particles/particulates are also distributed at various locations of the cast microstructure as shown in Fig. 3a–f.

XRD evaluation of the all combinations is showing an individual impact of all the powder particles with a major proportion of Al and Si. With an impact of processing, some amount of oxidation might be possible but very few peaks (almost negligible) are identified near a range of 47° as shown in Fig. 4. Influence of LM6 is also observed in form of present Si peaks at several locations, and near the major peaks just like Al powder, this confirms the domination of metal particles in solidification and un-melted behavior. Major peaks corresponding to Al and Si indicate the dominance of metal particles in solidification, with some peaks attributed to  $\text{Al}_2\text{O}_3$ . The presence of LM6 is indicated by Si peaks at various locations, corroborating its influence on the composite's properties. Despite potential oxidation, the XRD analysis suggests a correlation between processing effects and the observed properties and microstructure of the composite. Further refinement in XRD analysis could focus on identifying and quantifying the individual phases and elements present to provide a more comprehensive understanding of their contributions to the composite's properties.

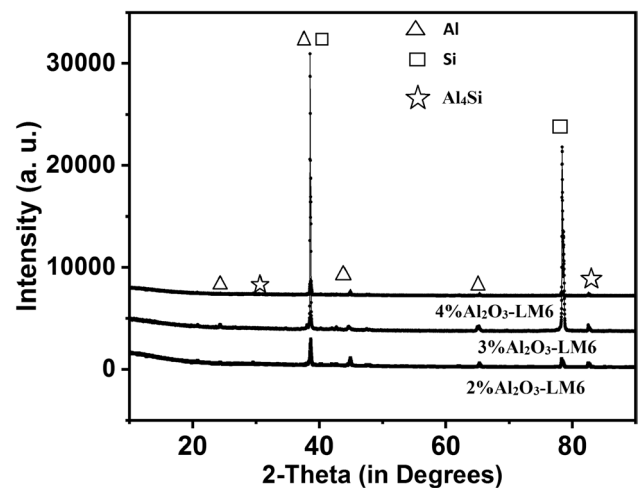


Fig. 4 XRD evaluation for synthesized  $\text{Al}_2\text{O}_3$ -LM6 composite

This effect of processing is representing a correlation with the properties and microstructure. Moreover, as shown in Table 1, hardness, and density represents a relation concerning  $\text{Al}_2\text{O}_3$  addition, and a continuous improvement is observed in these properties. As well as, less significant improvement is observed as a function of  $\text{Al}_2\text{O}_3$  for impact strength. Further, it was well obvious that self-pouring temperature should be increased with a rate of  $\text{Al}_2\text{O}_3$  addition and reaches a range of  $690.7^\circ\text{C}$  for 4%  $\text{Al}_2\text{O}_3$ -LM6 composite. In average, consolidated improvement of 1.4% for density and 9.9% for hardness is obtained for the effect of processing and reinforcement incorporation.

## Conclusions

- Development of  $\text{Al}_2\text{O}_3$  modified LM6 composite through self-pouring temperature route showcases potential enhancements in mechanical properties and cast microstructure.
- Successful integration of  $\text{Al}_2\text{O}_3$  and synthesis of the cast composite without conventional liquid slurry usage highlight promising results for a novel processing route.
- A composite blend comprising 83.5% Al, 12.5% Si, and 4%  $\text{Al}_2\text{O}_3$  demonstrates notable improvements in mechanical properties, including a 0.36% increase in density, 5.57% increase in hardness, and 5.23% increase in impact strength.
- Hardness and density measurements reflect functional enhancements attributed to reinforcement addition and underscore the effects of processing modifications.
- Despite the overall improvement, the impact strength of the developed composite remains a limiting factor.
- The microstructure analysis reveals a fine and uniform distribution of reinforcement particulates, along with silicon particles, contributing to the improved properties of the composite.

**Acknowledgements** The authors wish to express their gratitude to Mr. Abhilash Bajpai, Centre of Nano Sciences, IIT Kanpur and Materials Engineering laboratory staff of GLA University, Mathura for their experimental support.

**Funding** No any funding is received for this research work.

**Data Availability** The datasets obtained during and/or analyzed which is used in this experimental study, available from the corresponding author on required reasonable request.

## Declarations

**Conflict of interest** No potential conflict of interest was reported by the author(s).

## References

1. Z. Fan, Semisolid metal processing. *Int. Mater. Rev.* **47**(2), 49–85 (2002)
2. C. Morando, O. Fornaro, O. Garbellini, H. Palacio, Fluidity on metallic eutectic alloys. *Procedia Mater. Sci.* **8**, 959–967 (2015)
3. S. Alam, M.A. Chowdhury, Thermal gravimetric analysis of glass fiber reinforced composite for understanding the impact of copper oxide in relation to titanium oxide filler particles. *Compos. Theory Pract.* **21**, 1–2 (2021)
4. S. Suresh, G.H. Gowd, M.L.S. Deva-Kumar, Mechanical properties of AA 7075/ $\text{Al}_2\text{O}_3$ /SiC nano-metal matrix composites by stir-casting method. *J. Inst. Eng. India Ser.* **100**, 43–53 (2019)
5. D.P. Singh, V.K. Dwivedi, M. Agarwal, The key attributes of processing parameters on semi-solid metal casting: an overview, in *E3S Web of Conferences* (2021)
6. J. Xu, G. Chen, Z. Zhang, Y. Zhao, T. Zhang, C. Zhang, D. Ding, Effect of Al-3 wt%  $\text{Al}_2\text{O}_3$  master alloy fabricated by calcined kaolin on grain refinement and mechanical properties of A356 alloy. *J. Alloys Compd.* **862**, 158512 (2021)
7. M. Agarwal, R. Srivastava, Influence of fine  $\text{Al}_2\text{O}_3$  and aluminium nano-particles on the 6061 aluminium alloy near the grain boundary of the semi-solid cast microstructure. *Trans. Indian Ceram. Soc.* **78**(2), 94–100 (2019)
8. M. Agarwal, A. Singh, R. Srivastava, influence of powder-chip based reinforcement on tensile properties and fracture behaviors of LM6 aluminum alloy. *Trans. Indian Inst. Met.* **71**, 1091–1098 (2018)
9. M. Agarwal, R. Srivastava, Friction, wear and mechanical properties of Al-Si LM6 cast alloy processed in semi-solid stage. *SILICON* **11**, 355–366 (2019)
10. M. Karimian, A. Ourdjini, M.H. Idris, M. Bsher, A. Asmael, Effect of pouring temperature and melt treatment on microstructure of lost foam casting of Al-Si LM6 alloy. *Adv. Mater. Res.* **264–265**, 295–300 (2011)
11. V.B. Deev, K.V. Ponomareva, O.G. Prikhodko, S.V. Smetanyuk, Influence of temperatures of melt overheating and pouring on the quality of aluminum alloy lost foam castings. *Russ. J. Non-ferrous Metals* **58**, 373–377 (2017)
12. Y. Sui, K. Feng, C. Cheng, X. Chen, J. Qi, Y. He, Q. Meng, F. Wei, Z. Sun, Effects of pouring temperature on interfacial reaction between Ti-47.5Al-2.5V-1Cr alloy and mold during centrifugal casting. *J. Wuhan Univ. Technol. Mater. Sci. Edit.* **31**, 1105–1108 (2016)
13. J. Han, Z. Liu, Y. Jia, T. Wang, L. Zhao, J. Guo, Y. Chen, Effect of  $\text{TiB}_2$  addition on microstructure and fluidity of cast TiAl alloy. *Vacuum* **174**, 109210 (2020)
14. Y. Motoyama, H. Tokunaga, M. Yoshida, T. Maruyama, T. Okane, Measuring the interfacial heat transfer coefficient between flowing molten alloy and sand mold using fluidity tests. *J. Mater. Process. Technol.* **276**, 116394 (2020)
15. Y. Fu, H. Wang, C. Zhang, H. Hao, Effects of minor Sr additions on the as-cast microstructure, fluidity and mechanical properties of Mg-4.2Zn-1.7RE-0.8Zr-0.2Ca (wt%) alloy. *Mater. Sci. Eng. A* **723**, 118–125 (2018)
16. G. Mao, D. Liu, W. Gao, S. Liu, L. Zhong, The effects of copper (Cu) or zinc (Zn) on fluidity of A357 alloy. *Mater. Lett.* **304**, 130733 (2021)

17. L. Yang, W. Li, J. Du, K. Wang, P. Tang, Effect of Si and Ni contents on the fluidity of Al–Ni–Si alloys evaluated by using thermal analysis. *Thermochim. Acta* **645**, 7–15 (2016)
18. H. Huang, Y.X. Wang, P.H. Fu, L.M. Peng, H.Y. Jiang, W.Y. Xu, Fluidity of AZ91D and Mg–3Nd–0.2Zn–Zr (wt.%) magnesium alloys: response to pouring and mould temperature. *Int. J. Cast Metals Res.* **26**(4), 213–219 (2013)
19. Q. Zhang, M. Cao, J. Cai, AlSi9Mg aluminum alloy semi-solid slurry preparation by intermediate frequency electromagnetic oscillation process. *J. Mater. Process. Technol.* **215**, 42–49 (2019)
20. C. Carrasco, C. Camurri, J. García, C. Montalba, O. Prat, D. Rojas, Microstructure investigations and mechanical properties of an Al–Al<sub>2</sub>O<sub>3</sub> MMC produced by semi-solid solidification. *Mater. Sci. Eng. Technol.* **42**, 542–548 (2011)
21. N. Kumar, D. Khanduja, R.P. Singh, A study of mechanical properties on aluminum-based hybrid metal matrix composite (AA7175/B<sub>4</sub>C/SiC/Gr). *J. Inst. Eng. India Ser. D* **3**, 79 (2023)
22. H. Shin, K. Hong, Y. Yoo, W. Lee, Microstructure and oxidation behaviour of SiC fibre-reinforced Si<sub>3</sub>N<sub>4</sub>-AlN-Al<sub>2</sub>O<sub>3</sub>-Y<sub>2</sub>O<sub>3</sub> matrix composites. *Compos. Interfaces* **11**(5–6), 403–410 (2004)
23. P. Ashwath, M.A. Xavior, A.D. Batako, Processing, characterization, and properties of α-Al<sub>2</sub>O<sub>3</sub>-AA2900 composites for aerospace brake pad applications. *JOM* **73**, 4365–4375 (2021)
24. M. Agarwal, N.K. Dixit, M. Dixit, R. Srivastava, Interfacial study for the effect of Al<sub>2</sub>O<sub>3</sub> addition on the microstructure and micro-hardness of the Al<sub>2</sub>O<sub>3</sub>/AA6061 semi-solid cast composite. *Phase Trans.* **94**(12), 899–909 (2021)
25. S.S. Pungaiah, K.K. Sahu, R. Yuvaraja, G.J. Prabhu, R.R. Sudharsan, P. Thamizhvalavan, K. Ramaswamy, Investigation on mechanical behaviour of LM6 aluminum alloy hybrid composites processed using stir casting process. *Adv. Mater. Sci. Eng.* **7539546**, 7 (2022)
26. T.D.A. Saleh, Characteristics of oxide layer formed on the aluminium (LM6) alloy and aluminium (ADC12) alloy during in-situ melting. *J. Adv. Mech. Eng. Appl.* **2**(2), 61–73 (2021)
27. V.S. Kannan, K. Lenin, D. Srinivasan, D.R. Kumar, Analysis of microstructural, mechanical and surface properties of aluminium hybrid composites obtained through stir casting. *J. Inst. Eng. India Ser. D* (2023). <https://doi.org/10.1007/s40033-023-00512-8>

**Publisher’s Note** Springer Nature remains neutral with regard to jurisdictional claims in published maps and institutional affiliations.

Springer Nature or its licensor (e.g. a society or other partner) holds exclusive rights to this article under a publishing agreement with the author(s) or other rightsholder(s); author self-archiving of the accepted manuscript version of this article is solely governed by the terms of such publishing agreement and applicable law.